Astrophysics and Space Science
DOI 10.1007/s●●●●●-●●●-●●●●-●

A Systematic Study on Energy Dependence of Quasi-Periodic Oscillation Frequency in GRS 1915+105

Shu-Ping Yan[1,2,3,4] • Jin-Lu Qu[2,4] • Guo-Qiang Ding[1] • Peng Han [2,4] • Li-Ming Song[2,4] • Hong-Xing Yin[5] • Cheng-Min Zhang[6] • Shu Zhang [2,4] • Jian-Min Wang[2,4]

Abstract

Systematically studying all the *RXTE*/PCA observations for GRS 1915+105 before November 2010, we have discovered three additional patterns in the relation between Quasi-Periodic Oscillation (QPO) frequency and photon energy, extending earlier outcomes reported by Qu et al. (2010). We have confirmed that as QPO frequency increases, the relation evolves from the negative correlation to positive one. The newly discovered patterns provide new constraints on the QPO models.

Keywords accretion, accretion disks — black hole physics — stars: individual (GRS 1915+105) — stars: oscillations

Shu-Ping Yan

Jin-Lu Qu

Guo-Qiang Ding

Peng Han

Li-Ming Song

Hong-Xing Yin

Cheng-Min Zhang

Shu Zhang

Jian-Min Wang

[1]Xinjiang Astronomical Observatory, Chinese Academy of Sciences, 150, Science 1-Street, Urumqi, Xinjiang 830011, China; dinggq@uao.ac.cn, yanshup@uao.ac.cn

[2]Key Laboratory of Particle Astrophysics, Chinese Academy of Sciences, 19B Yuquan Road, Beijing 100049, China; qujl@ihep.ac.cn, songlm@ihep.ac.cn

[3]Graduate University of Chinese Academy of Sciences, 19A Yuquan road, Beijing 100049, China

[4]Opening Laboratory of Cosmic ray and High Energy Astrophysics, 19A Yuquan road, Beijing 100049, China

[5]School of Space Science and Physics, Shandong University, 264209, Weihai, China

[6]National Astronomical Observatoires, Chinese Academy of Sciences, 100012, Beijing, China

1 Introduction

GRS 1915+105, discovered by WATCH instrument on board *GRANAT* in 1992 (Castro-Tirado et al. 1992) and located in our galaxy at an estimated distance of 9 ± 3 kpc (Chapuis & Corbel 2004), is a low-mass X-ray binary containing a spinning accreting black hole (Zhang et al. 1997) of mass about 14 ± 4 $M_\odot$ and a K-M III giant star of mass 0.8 ± 0.5 $M_\odot$ as the donor (Harlaftis & Greiner 2004; Greiner et al. 2001a). The orbital separation and period of this binary are, respectively, about 108 ± 4 $R_\odot$ and 33.5 days (Greiner et al. 2001b). Serving as a famous microquasar, GRS 1915+105 produces superluminal radio jets (Mirabel & Rodriguez 1994; Fender et al. 1999). It shows various X-ray light curves and complex timing phenomena. Based on the appearance of light curves and color-color diagrams, the behaviors of GRS 1915+105 can be classified into 12 classes. The variability of the source can be further reduced to transitions between three basic states (A, B, and C) (Belloni et al. 2000). Of these 12 classes, class χ (state) is most commonly observed (Belloni et al. 2000). It shows characteristics exclusively of state C, the state which is steady in the X-rays and lies in a rather hard part of the color-color diagram. It is the state when the low-frequency ($\sim 0.5 - 10$ Hz) QPOs (LFQPOs) are most frequently observed (e.g., Muno et al. 1999), providing an idea site for studying LFQPOs.

Much effort has been made for exploring the origins of the LFQPOs of GRS 1915+105. It was found that the QPO frequency was positively correlated with the fluxes of the individual components and spectral total flux (e.g., Chen et al. 1997; Markwardt et al. 1999; Muno et al. 1999; Trudolyubov et al. 1999; Reig et al. 2000; Tomsick & Kaaret 2001). Muno et al. (2001) confirmed that QPO frequency was tightly correlated with the source flux, and, however, they also found

that for some observations the QPO frequency was not correlated with the flux. It was found that the QPO amplitude was inversely correlated with the source flux or QPO frequency (e.g., Muno et al. 1999; Reig et al. 2000; Trudolyubov et al. 1999). Muno et al. (1999) and Rodriguez et al. (2002a) reported that as QPO frequency increased, the temperature of the inner accretion disk increased and the radius of the inner accretion disk decreased. These results indicate that the LFQPO is linked to both the accretion disk and the region where the power law component is produced. However, most of these results are related to models. As a model-independent means, it is meaningful to study the correlations between photon energy and QPO parameters including its amplitude and frequency. Some authors found that the QPO amplitude increased with photon energy and it turned over in high energy bands in some cases (e.g., Tomsick & Kaaret 2001; Rodriguez et al. 2002b, 2004; Zdziarski et al. 2005). Qu et al. (2010) studied the LFQPOs of GRS 1915+105 in class χ state (Belloni et al. 2000) and found that as the centroid frequency of QPO increased the correlation between QPO frequency and photon energy evolved from a negative correlation to a positive one.

Nevertheless, systematic studies on the energy dependence of the LFQPO frequency in GRS 1915+105 have never been done. In this work, using all the data of *RXTE*/PCA of GRS 1915+105 before November 2010, we have investigated the correlation between photon energy and QPO frequency throughout. The data reduction methods are described in §2, the results are presented in §3, while a simple discussion and the conclusion are given in §4.

2 Observations and Data Reduction

We analyze all the *RXTE* observations of GRS 1915+105 before November, 2010, which are listed in Table 1. These observations are belonged to class χ state and with abundant LFOPOs (0.5–10 Hz) for evaluating the energy dependence of QPO frequency.

The light curves are extracted from the binned mode and event mode data of *RXTE*/PCA by using the HEASOFT version 6.7 package. Good time intervals are defined as follows: satellite elevation over the Earth limb $> 10^\circ$ and offset pointing $< 0.02^\circ$. In order to acquire the details of the correlations between photon energy and QPO frequency in broadband with enough confidence, only the generic binned configuration data with energy channel number ≥ 4 and time resolution ≤ 8 ms are selected. The light curves are extracted with a time resolution of 8 ms in PCA energy bands defined in Table 2. By running POWSPEC version 1.0 with "normalization = -2" option, the power density spectra (PDS) are produced with the normalization of Miyamoto et al. (1992), which gives the periodogram in units of $(\mathrm{rms/mean})^2/\mathrm{Hz}$, and corrected for Poisson noise (for details on PDS computation and X-ray PDS normalization practice, see, e.g., van der Klis 1989; Vaughan et al. 2003). The PDS are computated on an interval length of 64 s and Logarithmically rebinned by inputting -1.03 to rebin option. Following Belloni et al. (2002), we fit the PDS with a model including several Lorentzians to represent the QPOs, the continuum, and other broad features, respectively. The continuum of PDS can also be fitted with other models, for instance, a power law or a doubly broken power law (Belloni & Hasinger 1990). We have compared the quality of our current fits with that of the model including a power law for PDS continuum and several Lorentzians for other timing features and found that the multi-Lorentzian model fits better. A model consisting of a doubly broken power law plus several Lorentzians gives similar χ^2 values as our multi-Lorentzian fit. As pointed out by Belloni et al. (2002), the advantage of the multi-Lorentzian model fit is that it faciliates comparison across source types. Figure 1 shows an example of the five-Lorentzian fits of the PDS. The errors are derived by varying the parameters until $\Delta\chi^2 = 1$, at 1 σ level.

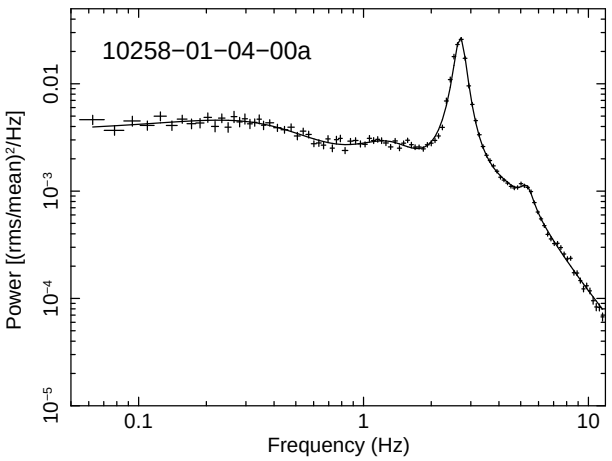

Fig. 1 An example of five-Lorentzian model fit of the PDS. The PDS are produced in PCA absolute channel 0-35.

3 Results

For each observation interval listed in Table 1, we have drawn a diagram that exhibits the relation between QPO frequency and photon energy. We use Least

Squares (see, e.g., Greene 2002) to estimate the linear correlation of the relations and obtain corresponding correlation coefficients (R), adjusted R-squares (R2) and slopes (k). Despite the complexity of the relations, they show some similar features. We find that it is possible to classify the relations into only six patterns, based on the appearance of the relation and the results of Least Squares fit. For the purpose of reducing the complexity of the amount of available data, we first focus on the relations with distinctive appearance and include them into corresponding patterns (see Table 1). Figure 2 shows three examples of energy-frequency relation for each pattern. In some cases, the QPO frequency decreases monotonously with energy, and R < -0.8, R2 > 0.6. We call this relation P1. Nevertheless, the relation is sometimes a positive "linear" correlation with R > 0.8, R2 > 0.6, which is referred to as P5. The other three patterns are the different combinations of P1 and P5. For P2, the frequency roughly maintains a constant at low energy and decreases with the energy at high energy. For P3, the relation evolves from a positive correlation (P5) to a negative one (P1) as the energy increases. While for P4, the frequency increases with energy at low energy and then it approximates a constant at high energy. The remaining relations are irregular/indistinct and hard to be included into certain patterns mentioned above. We call them P0. The P1 and P5 were firstly found by Qu et al. (2010), while P2, P3, P4 were newly discovered.

The correlation coefficients and adjusted R-squares of each pattern are shown in Figure 3. It is clear that P1 and P5 possess significant linear correlation, P3 nonlinear correlation, while P2, P4 being mediate. The P0 points scatter among the points of P2, P3 and P4. In the order of P1 → P2 → P3 → P4 → P5, the correlation coefficients increase gradually from ∼ -1 to ∼ 1. This supports our classification as optimal.

Generally, with increasing of the QPO frequency and source intensity, the relation evolves from P1 to P5, via P2, P3 and P4, as demonstrated by Figure 4: the averaged QPO frequencies and intensities of P1 and P2 are obviously lower than those of P3, P4, and P5; the cases when QPO frequency $f \gtrsim 5$ Hz or count rate $\gtrsim 3000$ cts/s/PCU2 only occur in P5 and all the count rates and QPO frequencies of P1 and P2 are, respectively, less than ∼2000 cts/s/PCU2 and ∼4 Hz.

The relation between QPO frequency and the slope is shown in Figure 5. Panel (a) of Figure 5 demonstrates the slopes of P1 (k < 0, f < 3 Hz) and P5 (k > 0, f > 2 Hz). It is clearly that as QPO frequency increases, the relation between QPO frequency and photon energy evolves from the negative correlation (P1) to the positive one (P5). Panel (b) of Figure

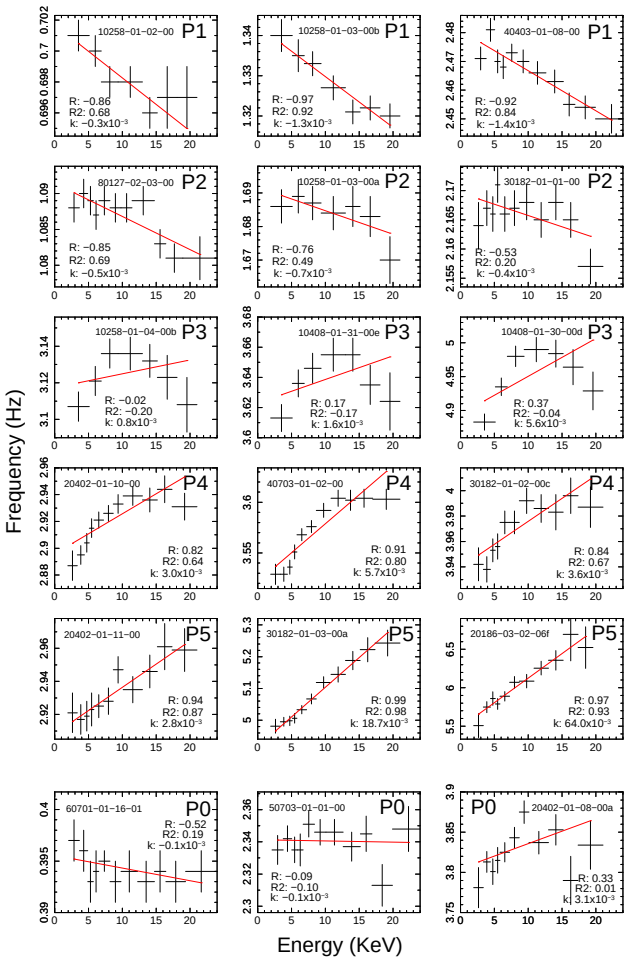

Fig. 2 Three examples of frequency-energy relation for each pattern. The horizontal bars are band widths, and the vertical bars are error bars. The relations are fitted with Least Squares and the red oblique lines are the Best Fitting Lines. "R" denotes correlation coefficient, "R2" denotes adjusted R-square and "k" denotes the slope of the fitting line. P1: the QPO frequency decreases monotonously with energy, R < -0.8, R2 > 0.6; P2: the frequency roughly maintains a constant at low energy and decreases with the energy at high energy; P3: the relation evolves from a positive correlation to a negative one as the energy increases; P4: the QPO frequency increases with energy at low energy and then it approximates a constant at high energy; P5: the QPO frequency increases monotonously with energy, R > 0.8, R2 > 0.6. P0: the irregular/indistinct relations.

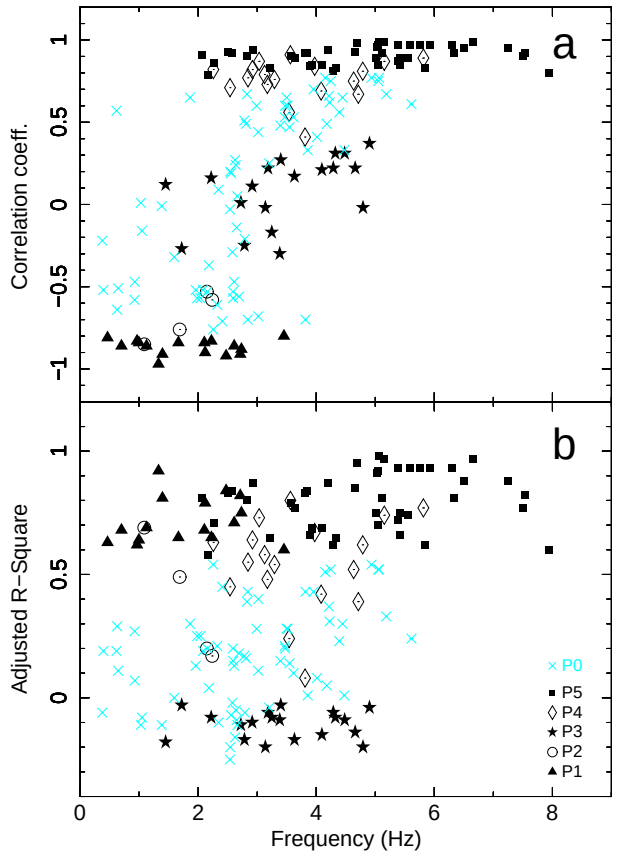

Fig. 3 The QPO frequencies versus the correlation coefficients (a) and the adjusted R-squares (b) of six patterns. The triangles are observation intervals whose energy-frequency relations are belong to P1, the circles P2, the pentagons P3, the diamond P4, the squares P5, and the cyan crosses P0.

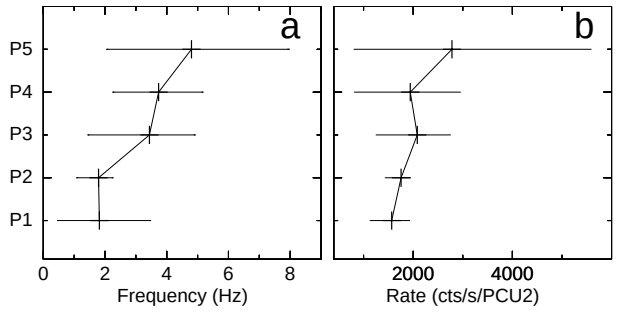

Fig. 4 The QPO frequency statistics (a) and source count rate statistics (b) for five patterns of the relation between QPO frequency and photon energy. The solid horizontal lines denotes the width of the band where QPO frequency or count rate measurements fall. The crosses denotes the averaged QPO frequency or count rate of observation intervals of each pattern.

5 demonstrates the slopes of all (168) observation intervals listed in Table 1. The track in panel (b) is similar to that in panel (a), which confirms the evolution from P1 to P5, via P2, P3 and P4. This also suggests that our patterns are representative.

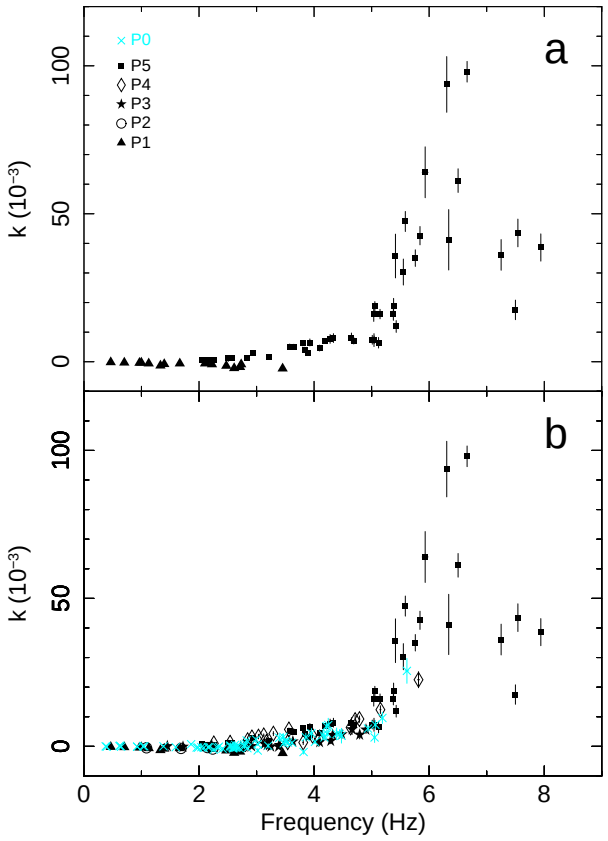

Fig. 5 (a) the relation between QPO frequencies and the slopes of P1 and P5. (b) the relation between QPO frequencies and the slopes (k) of all (168) observations listed in Table 1. The horizontal and vertical bars are error bars. Some error bars are smaller than the symbols. The triangles are observation intervals whose energy-frequency relations are belong to P1, the circles P2, the pentagons P3, the diamond P4, the squares P5, and the cyan crosses P0.

4 Discussion and Conclusions

By systematically analyzing all the *RXTE*/PCA observations of GRS 1915+105 before November 2010, we have found that there are five typical patterns of the relation between QPO frequency and photon energy: the negative correlation (P1) and the positive one (P5), as well as three combined relations of them (P2, P3 and P4). The P1 and P5 were firstly found by Qu et al. (2010) and the intermediate patterns, P2, P3 and P4, were newly discovered in this work. Besides, we have confirmed in large sample the result reported

by Qu et al. (2010): with increasing of the centroid frequency of QPO, the relation between QPO frequency and photon energy evolves from P1 to P5.

Following Qu et al. (2010), we apply several models to the detected patterns between the QPO frequency and photon energy. Titarchuk & Osherovich (2000) proposed the global disk model (GDM) to interpret the LFQPOs in X-ray binaries, in which they argued that the disk oscillations were the result of gravitational interaction between the the central compact objects and the disk and the QPO frequency was determined by the mass of the central object. Thus, the QPO frequency determined by the GDM is expected to be independent of the photon energy and therefore, this model can explain those QPOs whose coefficients are zero, as demonstrated in bottom panel of Figure 5. The radial and orbital oscillation model (ROOM) is a typical model for QPOs (Nowak & Wagoner 1993; Nowak 1994). According to this model, the oscillation frequency will vary with the the disk radius or temperature, resulting in that the QPO frequency will vary with the photon energy, because photons with different energies are from different radii. Simply assuming the disk oscillation frequency to be the Keplerian frequency at the inner disk radius, it is natural to explain the relation P5: with decreasing of the inner disk radius, the QPO frequency increases, and meanwhile the photon energy increases, because the temperature at inner disk edge also increases. Fortunately, Muno et al. (1999) reported that in this source the QPO parameters were indeed correlated with the disk parameters. Other models such as the drift blob model (DBM; Böttcher & Liang 1998, 1999) can also be used to explain the energy dependence of QPO frequency. In the DBM, the blobs drifting inward through an inhomogeneous hot inner disk or corona would cause the QPO frequency to increase with energy. Both the ROOM and DBM can explain the positive correlation between the QPO frequency and photon energy, but they are frustrated by the negative correlation (P1) and other complicated correlations (P2, P3, and P4). There is no model for interpreting all the relations, which perhaps indicates that the QPOs with different relations between the QPO frequency and photon energy result from different mechanisms.

This work presents various patterns of relation between the QPO frequency and photon energy in the famous microquasar GRS 1915+105, indicating that the mechanisms for QPOs are complicated. On the other hands, we extend the investigation on the relations made by Qu et al. (2010) and the newly discovered relations provide new clues on QPO models.

Acknowledgements

The authors thank the anonymous referee for some helpful suggestions and comments. This research has made use of data obtained through the High Energy Astrophysics Science Archive Research Center (HEASARC) On-line Service, provided by NASA/ Goddard Space Flight Center (GSFC). This work is partially supported by the Natural Science Foundation of Xinjiang Uygur Autonomous Region of China (Grant No. 200821164), the Program of the Light in Chinese Western Region (LCWR) (Grant No. LHXZ 200802) provided by Chinese Academy of Sciences (CAS), the National Basic Research Program of China (973 Program 2009CB824800), the Natural Science Foundation of China (Grant No. 10733010, 11073021, 10325313, 10521001 and 10773017) and the Natural Science Foundation of China for Young Scientists (Grant No. 10903005).

References

Belloni, T., Hasinger, G.: A&A **227**, L33 (1990)
Belloni, T., Klein-Wolt, M., Méndez, M., van der Klis, M., van Paradijs, J.: A&A **355**, 271 (2000)
Belloni, T., Psaltis, D., van der Klis, M.: ApJ **572**, 392 (2002)
Böttcher, M., Liang, E.P.: ApJ **506**, 281 (1998)
Böttcher, M., Liang, E.P.: ApJ **511**, L37 (1999)
Castro-Tirado, A.J., Brandt, S., Lund, N.: IAUC **5590**, 2 (1992)
Chapuis, C., Corbel, S.: A&A **414**, 659 (2004)
Chen, X., Swank, J.H., Taam, R.E.: ApJ **477**, L41 (1997)
Fender, R.P., Garrington, S.T., McKay, D.J. et al.: MNRAS **304**, 865 (1999)
Greene, W.H.: Econometric Analysis (5th ed.) **Prentice Hall**, P. 34 (2002)
Greiner, J., Cuby, J.G., McCaughrean, M.J. et al.: A&A **373**, L37 (2001a)
Greiner, J., Cuby, J.G., McCaughrean, M.J.: Nature **414**, 522 (2001b)
Harlaftis, E.T., Greiner, J.: A&A **414**, L13 (2004)
Markwardt, C.B., Swank, J.H., Taam, R.E.: ApJ **513**, L37 (1999)
Mirabel, I.F., Rodriguez, L.F.: Nature **371**, 46 (1994)
Miyamoto, S., Kitamoto, S., Iga, S., Negoro, H., Terada, K.: ApJ **391**, L21 (1992)
Muno, M.P., Morgan, E.H., Remillard, R.A.: ApJ **527**, 321 (1999)
Muno, M.P., Remillard, R.A., Morgan, E.H.: ApJ **556**, 515 (2001)
Nowak, M.A.: ApJ **422**, 688 (1994)
Nowak, M.A., Wagoner, R.V.: ApJ **418**, 187 (1993)
Qu, J.L., Lu, F.J., Zhang, S., Ding, G.Q., Wang, J.M.: ApJ **710**, 836 (2010)
Reig, P., Belloni, T., van der Klis, M. et al.: ApJ **541**, 883 (2000)
Rodriguez, J., Corbel, S., Hannikainen, D.C. et al.: ApJ **615**, 416 (2004)
Rodriguez, J., Varniére, P., Tagger, M., Durouchoux, Ph.: A&A **387**, 487 (2002a)
Rodriguez, J., Durouchoux, P., Mirabel, F. et al.: A&A **386**, 271 (2002b)
Titarchuk, L., Osherovich, V.: ApJ **542**, L111 (2000)
Tomsick, J.A., Kaaret, P.: ApJ **548**, 401 (2001)
Trudolyubov, S., Churazov, E., Gilfanov, M.: Astron. Lett. **25**, 718 (1999)
van der Klis, M.: ARA&A **27**, 517 (1989)
Vaughan, S., Edelson, R., Warwick, R.S., Uttley, P.: MNRAS **345**, 1271 (2003)
Zdziarski, A.A., Gierlinski, M., Rao, A.R. et al.: MNRAS **360**, 825 (2005)
Zhang, S.N., Cui, W., Chen, W.: ApJ **482**, L155 (1997)

Table 1 The *RXTE* Observations of GRS 1915+105 Reduced in This Paper and The Results

					QPO			Energy–Frequency				
ObsID	Date	GTI[a] (s)	Rate[b]	ChID[c]	Frequency (Hz)	χ^2	Q[d]	P[e]	k^f ($\times 10^{-3}$)	χ^2	R[g]	R2[h]
10258-01-02-00	29/07/96	9160	1739	Ch1E3	0.699 ± 0.001	2.16	6.9 ± 0.4	P1	-0.3 ± 0.1	0.65	-0.86	0.68
10258-01-03-00a	06/08/96	3328	1757	Ch1E3	1.687 ± 0.004	3.22	6.3 ± 0.3	P2	-0.7 ± 0.4	0.52	-0.76	0.49
10258-01-03-00b	06/08/96	3360	1771	Ch1E3	1.329 ± 0.003	2.08	9.8 ± 0.7	P1	-1.3 ± 0.2	0.52	-0.97	0.92
10258-01-03-00c	06/08/96	3360	1736	Ch1E3	1.450 ± 0.004	1.82	8.5 ± 0.5	P3	-0.0 ± 0.3	1.55	0.12	-0.18
10258-01-04-00a	14/08/96	6800	1915	Ch1E3	2.692 ± 0.003	1.87	7.2 ± 0.2	P0	-0.4 ± 0.3	1.85	-0.56	0.18
10258-01-04-00b	14/08/96	3408	1971	Ch1E3	3.129 ± 0.007	2.14	6.5 ± 0.2	P3	0.8 ± 0.7	1.90	-0.02	-0.20
10258-01-05-00a	20/08/96	2688	3743	Ch2E3	6.339 ± 0.027	1.96	3.4 ± 0.2	P5	41.2 ± 10.2	1.81	0.92	0.81
10258-01-05-00b	20/08/96	3376	3750	Ch2E3	6.305 ± 0.021	2.65	3.8 ± 0.2	P5	93.7 ± 9.4	0.47	0.97	0.93
10258-01-06-00a	29/08/96	1400	5549	Ch2E3	7.250 ± 0.040	1.28	6.8 ± 1.0	P5	36.1 ± 5.2	2.10	0.95	0.88
10258-01-06-00b	29/08/96	3408	5587	Ch2E3	7.527 ± 0.027	1.20	7.5 ± 1.0	P5	17.5 ± 3.3	1.71	0.90	0.77
10408-01-22-00	11/07/96	3328	2122	Ch2E3	3.473 ± 0.005	0.88	10.1 ± 0.5	P0	1.0 ± 0.6	0.95	0.60	0.20
10408-01-22-01	11/07/96	3312	2020	Ch2E3	2.785 ± 0.005	2.31	7.1 ± 0.2	P3	-0.1 ± 0.6	1.09	-0.25	-0.17
10408-01-22-02a	11/07/96	1600	1989	Ch2E3	2.545 ± 0.008	2.08	7.7 ± 0.5	P0	0.3 ± 0.9	0.46	0.20	-0.20
10408-01-22-02b	11/07/96	820	1954	Ch2E3	2.507 ± 0.008	2.08	8.5 ± 0.8	P5	1.1 ± 1.0	0.05	0.93	0.83
10408-01-22-02c	11/07/96	892	1929	Ch2E3	2.625 ± 0.009	2.08	8.2 ± 0.6	P0	0.5 ± 1.1	0.48	0.27	-0.16
10408-01-23-00a	14/07/96	3167	2109	Ch2E3	3.499 ± 0.006	1.90	7.3 ± 0.2	P0	1.7 ± 0.7	1.71	0.65	0.28
10408-01-23-00b	14/07/96	3312	2108	Ch2E3	3.615 ± 0.005	1.76	8.7 ± 0.3	P0	1.2 ± 0.6	1.50	0.53	0.10
10408-01-23-00c	14/07/96	3257	2255	Ch2E3	4.179 ± 0.008	1.50	6.3 ± 0.2	P0	3.0 ± 1.0	3.02	0.49	0.05
10408-01-24-00a	16/07/96	2447	1949	Ch2E3	2.238 ± 0.006	2.36	8.1 ± 0.5	P2	-0.9 ± 0.5	2.19	-0.58	0.17
10408-01-24-00b	16/07/96	3312	1943	Ch2E3	2.324 ± 0.005	2.60	7.2 ± 0.3	P0	-0.5 ± 0.5	0.53	-0.61	0.21
10408-01-24-00c	16/07/96	2953	1952	Ch2E3	2.537 ± 0.005	2.34	9.4 ± 0.5	P0	-0.0 ± 0.5	0.35	-0.03	-0.25
10408-01-24-00d	16/07/96	913	1965	Ch2E3	2.594 ± 0.008	1.59	11.0 ± 0.8	P0	-0.7 ± 0.8	0.57	-0.57	0.15
10408-01-25-00	19/07/96	9952	1820	Ch1E3	1.126 ± 0.002	3.34	6.3 ± 0.2	P1	-0.6 ± 0.2	1.45	-0.86	0.69
10408-01-27-00a	26/07/96	2336	1783	Ch1E3	0.645 ± 0.002	1.43	7.6 ± 0.9	P0	-0.1 ± 0.1	0.42	-0.51	0.11
10408-01-27-00b	26/07/96	3296	1791	Ch1E3	0.617 ± 0.002	1.20	7.3 ± 0.6	P0	0.1 ± 0.2	0.21	0.57	0.19
10408-01-27-00c	26/07/96	3296	1769	Ch1E3	0.629 ± 0.002	1.23	6.1 ± 0.5	P0	0.2 ± 0.2	0.26	-0.64	0.29
10408-01-28-00a	03/08/96	3328	1742	Ch1E3	0.996 ± 0.002	1.60	8.5 ± 0.6	P1	-0.3 ± 0.2	0.53	-0.84	0.64
10408-01-28-00b	03/08/96	3328	1744	Ch1E3	0.965 ± 0.004	2.14	8.9 ± 0.6	P1	-0.4 ± 0.2	0.22	-0.83	0.62
10408-01-28-00c	03/08/96	3328	1731	Ch1E3	0.927 ± 0.003	1.24	7.8 ± 0.5	P0	-0.1 ± 0.2	0.33	-0.47	0.07
10408-01-29-00a	10/08/96	2965	1760	Ch1E3	1.665 ± 0.004	1.66	10.1 ± 0.6	P1	-0.6 ± 0.3	0.33	-0.84	0.65
10408-01-29-00b	10/08/96	3392	1784	Ch1E3	1.863 ± 0.004	2.38	8.9 ± 0.5	P0	0.7 ± 0.3	0.63	0.65	0.30
10408-01-29-00c	10/08/96	3392	1787	Ch1E3	1.960 ± 0.004	2.80	9.4 ± 0.5	P0	-0.4 ± 0.3	0.55	-0.52	0.13
10408-01-30-00a	18/08/96	1696	2388	Ch1E3	4.323 ± 0.012	2.13	5.8 ± 0.3	P3	3.8 ± 1.4	4.68	0.31	-0.08
10408-01-30-00b	18/08/96	1696	2588	Ch1E3	4.792 ± 0.011	1.36	7.1 ± 0.4	P3	3.9 ± 1.4	6.32	-0.02	-0.20
10408-01-30-00c	18/08/96	1696	2842	Ch1E3	5.187 ± 0.017	1.38	6.2 ± 0.4	P0	9.6 ± 1.9	2.44	0.67	0.33
10408-01-30-00d	18/08/96	1696	2752	Ch1E3	4.901 ± 0.011	1.06	7.7 ± 0.7	P3	5.6 ± 1.3	5.15	0.37	-0.04
10408-01-30-00e	18/08/96	1688	2986	Ch1E3	5.427 ± 0.015	1.00	8.6 ± 0.7	P5	11.9 ± 2.0	1.92	0.85	0.66
10408-01-31-00a	25/08/96	2319	2327	Ch1E3	4.096 ± 0.006	1.15	9.3 ± 0.5	P3	1.4 ± 0.6	2.83	0.21	-0.15
10408-01-31-00b	25/08/96	1000	2555	Ch1E3	4.660 ± 0.015	1.31	8.2 ± 0.7	P3	5.7 ± 1.7	3.93	0.22	-0.14
10408-01-31-00c	25/08/96	1328	2496	Ch1E3	4.482 ± 0.014	1.30	7.2 ± 0.4	P3	4.0 ± 1.4	4.38	0.31	-0.09
10408-01-31-00d	25/08/96	1000	2323	Ch1E3	4.154 ± 0.014	1.32	8.2 ± 0.7	P0	4.0 ± 1.3	1.25	0.77	0.51
10408-01-31-00e	25/08/96	1664	2133	Ch1E3	3.630 ± 0.009	1.58	7.4 ± 0.4	P3	1.6 ± 0.8	2.07	0.17	-0.17
10408-01-31-00f	25/08/96	1664	2057	Ch1E3	3.382 ± 0.008	1.52	9.7 ± 0.5	P3	-0.1 ± 0.7	3.09	-0.30	-0.09
10408-01-32-00a	31/08/96	2912	4239	Ch1E3	6.503 ± 0.026	2.53	4.6 ± 0.6	P5	61.2 ± 4.0	2.33	0.95	0.88
10408-01-32-00b	31/08/96	3312	3648	Ch1E3	5.840 ± 0.017	2.19	7.0 ± 0.7	P5	42.6 ± 3.1	2.65	0.83	0.62
10408-01-32-00c	31/08/96	1170	3314	Ch1E3	5.613 ± 0.032	1.17	5.7 ± 0.5	P0	25.5 ± 4.2	2.31	0.61	0.24
10408-01-33-00a	07/09/96	912	3527	Ch1E3	5.550 ± 0.030	1.67	5.2 ± 0.6	P5	30.3 ± 4.4	1.30	0.89	0.74
10408-01-33-00b	07/09/96	2495	3743	Ch1E3	5.586 ± 0.017	1.68	7.4 ± 0.8	P5	47.4 ± 3.4	2.87	0.97	0.93
10408-01-33-00c	07/09/96	1295	3655	Ch1E3	5.414 ± 0.039	1.91	3.8 ± 0.4	P5	35.7 ± 7.4	0.23	0.89	0.75
10408-01-42-00a	23/10/96	3312	3289	Ch1E3	5.044 ± 0.009	2.49	8.2 ± 0.4	P5	7.4 ± 1.3	1.08	0.97	0.92
10408-01-42-00b	23/10/96	3312	2921	Ch1E3	4.690 ± 0.009	2.45	7.1 ± 0.3	P5	7.1 ± 1.1	0.73	0.98	0.95
10408-01-43-00a	23/10/96	2416	3274	Ch1E3	5.011 ± 0.010	2.14	8.3 ± 0.5	P5	7.4 ± 1.5	2.09	0.89	0.75
10408-01-43-00b	23/10/96	2284	3314	Ch1E3	5.064 ± 0.012	1.86	8.1 ± 0.4	P0	7.3 ± 1.5	2.99	0.77	0.52
10408-01-43-00c	23/10/96	1980	3302	Ch1E3	5.121 ± 0.013	1.90	7.3 ± 0.4	P5	6.4 ± 1.8	1.44	0.92	0.81
10408-01-43-00d	23/10/96	1740	2709	Ch1E3	4.446 ± 0.013	1.43	6.7 ± 0.4	P0	4.2 ± 1.5	0.73	0.65	0.30
20186-03-02-052a	17/09/97	3031	3096	Ch3E3	5.381 ± 0.019	1.63	7.5 ± 0.7	P5	18.8 ± 2.6	1.82	0.87	0.72
20186-03-02-052b	17/09/97	3031	3203	Ch3E3	5.759 ± 0.018	2.11	4.7 ± 0.2	P5	35.0 ± 2.8	2.27	0.97	0.93
20186-03-02-052c	17/09/97	3312	2348	Ch3E3	4.083 ± 0.006	1.73	7.9 ± 0.3	P4	2.6 ± 0.6	2.73	0.69	0.42
20186-03-02-052d	17/09/97	3312	2563	Ch3E3	4.633 ± 0.008	1.37	6.8 ± 0.2	P4	6.4 ± 0.9	3.09	0.75	0.52
20186-03-02-052e	17/09/97	3312	2802	Ch3E3	5.153 ± 0.011	1.52	7.3 ± 0.4	P4	12.4 ± 1.3	3.44	0.87	0.74
20186-03-02-060a	18/09/97	2768	2852	Ch3E3	5.036 ± 0.021	2.07	4.8 ± 0.3	P5	16.1 ± 2.5	0.79	0.96	0.91
20186-03-02-060b	18/09/97	9936	4385	Ch3E3	6.658 ± 0.031	2.26	2.4 ± 0.1	P5	98.0 ± 3.5	1.92	0.99	0.97
20186-03-02-060c	18/09/97	3312	2679	Ch3E3	4.788 ± 0.011	1.34	5.7 ± 0.2	P4	9.2 ± 1.1	3.99	0.81	0.62
20186-03-02-06a	18/09/97	1656	2767	Ch3E3	5.042 ± 0.017	1.17	5.1 ± 0.3	P5	7.3 ± 2.2	0.65	0.85	0.70
20186-03-02-06b	18/09/97	1656	2430	Ch3E3	4.226 ± 0.013	1.33	7.1 ± 0.3	P0	4.3 ± 1.1	2.72	0.62	0.31
20186-03-02-06c	18/09/97	1600	2255	Ch3E3	3.810 ± 0.008	1.13	8.2 ± 0.4	P4	1.3 ± 0.7	1.69	0.41	0.08
20186-03-02-06d	18/09/97	1695	2399	Ch3E3	4.288 ± 0.009	1.49	7.8 ± 0.4	P3	1.8 ± 0.9	1.89	0.22	-0.06
20186-03-02-06e	18/09/97	1550	2761	Ch3E3	5.051 ± 0.013	0.70	7.3 ± 0.5	P0	3.0 ± 1.7	0.56	0.75	0.52
20186-03-02-06f	18/09/97	1569	3648	Ch3E3	5.930 ± 0.050	1.35	2.6 ± 0.2	P5	64.0 ± 8.6	0.40	0.97	0.93
20402-01-05-00	05/12/96	2048	1421	Ch5E3	2.825 ± 0.004	1.89	6.1 ± 0.2	P5	1.2 ± 0.3	0.34	0.90	0.80
20402-01-06-00a	11/12/96	3312	1360	Ch5E3	3.034 ± 0.009	1.00	5.0 ± 0.3	P4	3.3 ± 0.8	0.77	0.87	0.73
20402-01-06-00b	11/12/96	3312	1279	Ch5E3	2.844 ± 0.007	1.31	5.6 ± 0.3	P4	2.1 ± 0.6	1.46	0.77	0.55
20402-01-06-00c	11/12/96	2780	1211	Ch5E3	2.568 ± 0.007	1.42	5.7 ± 0.3	P5	1.2 ± 0.6	0.08	0.92	0.84
20402-01-07-00	19/12/96	9296	1310	Ch5E3	3.125 ± 0.005	1.48	4.2 ± 0.1	P4	3.7 ± 0.5	2.54	0.79	0.58
20402-01-08-00a	24/12/96	2658	1318	Ch5E3	3.845 ± 0.010	1.63	5.1 ± 0.2	P0	3.1 ± 1.3	2.09	0.33	0.01
20402-01-08-00b	24/12/96	2834	1325	Ch5E3	3.927 ± 0.010	2.27	5.0 ± 0.2	P5	6.5 ± 1.2	1.36	0.85	0.69
20402-01-08-01	25/12/96	3312	1232	Ch5E3	3.465 ± 0.009	1.25	4.4 ± 0.2	P0	3.2 ± 1.1	1.54	0.53	0.21
20402-01-09-00	31/12/96	7548	1099	Ch5E3	2.827 ± 0.005	1.87	5.1 ± 0.2	P0	2.0 ± 0.5	1.46	0.67	0.39
20402-01-10-00	08/01/97	9804	993	Ch5E3	2.920 ± 0.005	2.22	4.8 ± 0.2	P4	3.0 ± 0.5	1.84	0.82	0.64
20402-01-11-00	14/01/97	6519	912	Ch5E3	2.930 ± 0.006	1.33	5.2 ± 0.2	P5	2.8 ± 0.7	0.42	0.94	0.87
20402-01-12-00a	23/01/97	5695	883	Ch5E3	2.811 ± 0.006	1.60	5.3 ± 0.3	P0	0.9 ± 0.7	0.86	0.49	0.16

Table 1—Continued

					QPO			Energy–Frequency				
ObsID	Date	GTI[a] (s)	Rate[b]	ChID[c]	Frequency (Hz)	χ^2	Q[d]	P[e]	k^f ($\times 10^{-3}$)	χ^2	R[g]	R2[h]
20402-01-12-00b	23/01/97	3755	894	Ch5E3	2.790 ± 0.007	1.50	6.0 ± 0.4	P0	0.0 ± 0.8	0.91	-0.21	-0.06
20402-01-13-00	29/01/97	10000	936	Ch5E3	3.649 ± 0.007	1.57	4.0 ± 0.1	P5	5.0 ± 0.9	1.64	0.89	0.77
20402-01-14-00	01/02/97	9394	910	Ch5E3	3.577 ± 0.007	2.58	4.0 ± 0.1	P5	5.1 ± 0.9	1.46	0.90	0.79
20402-01-15-00	09/02/97	10222	816	Ch5E3	2.258 ± 0.004	2.14	5.9 ± 0.2	P4	1.0 ± 0.4	0.43	0.82	0.63
20402-01-16-00	22/02/97	5951	803	Ch5E3	2.991 ± 0.007	1.49	5.4 ± 0.3	P0	2.3 ± 0.7	2.59	0.60	0.28
20402-01-20-00	17/03/97	7300	807	Ch5E3	3.217 ± 0.006	1.19	5.4 ± 0.2	P5	1.7 ± 0.7	0.72	0.83	0.65
20402-01-26-00a	25/04/97	2220	1137	Ch5E3	3.954 ± 0.012	1.47	4.9 ± 0.3	P0	4.4 ± 1.6	1.13	0.70	0.43
20402-01-26-00b	25/04/97	2884	1188	Ch5E3	4.279 ± 0.011	2.19	4.7 ± 0.2	P5	7.7 ± 1.5	1.52	0.81	0.62
20402-01-26-00c	25/04/97	3300	1210	Ch5E3	4.475 ± 0.016	1.82	3.6 ± 0.2	P0	3.6 ± 2.5	0.77	0.33	0.01
20402-01-26-00d	25/04/97	3328	1178	Ch5E3	4.246 ± 0.017	1.68	3.5 ± 0.2	P0	7.2 ± 2.3	0.66	0.75	0.52
20402-01-26-00e	25/04/97	1964	1163	Ch5E3	4.391 ± 0.014	2.08	4.8 ± 0.2	P0	4.2 ± 2.0	1.77	0.56	0.23
20402-01-48-00a	29/09/97	3296	4714	Ch5E3	7.541 ± 0.038	1.54	5.2 ± 0.4	P5	43.5 ± 4.7	1.99	0.92	0.82
20402-01-48-00b	29/09/97	3328	2726	Ch5E3	4.713 ± 0.014	1.73	5.7 ± 0.4	P4	8.9 ± 1.6	3.93	0.67	0.39
20402-01-50-01	16/10/97	4994	1497	Ch5E3	1.048 ± 0.003	2.39	8.2 ± 0.5	P0	-0.0 ± 0.2	0.40	-0.16	-0.08
20402-01-51-00	22/10/97	9399	1490	Ch5E3	1.396 ± 0.002	3.47	7.8 ± 0.2	P1	-0.8 ± 0.1	0.71	-0.91	0.81
30182-01-01-00	08/07/98	11606	1435	Ch3E3	2.148 ± 0.003	2.36	5.7 ± 0.2	P2	-0.4 ± 0.2	0.97	-0.53	0.20
30182-01-02-00a	09/07/98	5073	1889	Ch3E3	3.247 ± 0.005	1.94	7.7 ± 0.3	P3	-0.1 ± 0.4	0.62	-0.17	-0.08
30182-01-02-00b	09/07/98	3359	2069	Ch3E3	3.541 ± 0.006	2.23	7.3 ± 0.3	P4	1.4 ± 0.6	1.95	0.56	0.24
30182-01-02-00c	09/07/98	2968	2466	Ch3E3	3.973 ± 0.008	2.89	6.0 ± 0.3	P4	3.6 ± 0.8	1.17	0.84	0.67
30182-01-03-00a	10/07/98	3344	3479	Ch3E3	5.056 ± 0.013	2.19	6.4 ± 0.3	P5	18.7 ± 1.6	0.43	0.99	0.98
30182-01-03-00b	10/07/98	2472	3677	Ch3E3	5.147 ± 0.010	2.77	9.3 ± 0.6	P5	16.1 ± 1.6	0.69	0.99	0.97
30182-01-04-00a	11/07/98	1678	2360	Ch3E3	4.096 ± 0.010	1.46	7.0 ± 0.5	P5	4.6 ± 1.0	1.03	0.85	0.69
30182-01-04-00b	11/07/98	4166	1933	Ch3E3	3.400 ± 0.006	2.18	7.4 ± 0.3	P3	0.4 ± 0.5	0.98	0.27	-0.03
30182-01-04-00c	11/07/98	3328	1709	Ch3E3	2.916 ± 0.006	2.25	9.1 ± 0.4	P3	0.0 ± 0.4	1.21	0.11	-0.10
30182-01-04-00d	11/07/98	3324	1604	Ch3E3	2.664 ± 0.005	1.87	9.0 ± 0.4	P0	-0.2 ± 0.4	1.55	0.05	-0.11
30182-01-04-01a	12/07/98	2236	1581	Ch3E3	2.652 ± 0.006	1.44	8.8 ± 0.5	P0	-0.3 ± 0.4	1.09	-0.14	-0.09
30182-01-04-01b	12/07/98	2728	1513	Ch3E3	2.410 ± 0.005	1.61	7.6 ± 0.3	P0	-0.8 ± 0.4	0.52	-0.71	0.45
30182-01-04-01c	12/07/98	3340	1605	Ch3E3	2.725 ± 0.006	1.70	7.4 ± 0.3	P3	-0.1 ± 0.5	0.83	0.01	-0.11
30182-01-04-01d	12/07/98	3340	2010	Ch3E3	3.392 ± 0.014	2.64	4.3 ± 0.2	P0	2.9 ± 1.2	1.51	0.48	0.15
30182-01-04-01e	12/07/98	2400	2665	Ch3E3	4.215 ± 0.010	2.74	6.6 ± 0.3	P0	6.8 ± 1.1	4.76	0.66	0.37
30402-01-09-01	10/04/98	2546	1979	Ch6E3	2.157 ± 0.004	2.84	8.9 ± 0.4	P0	-0.3 ± 0.3	0.42	-0.53	0.20
30402-01-10-00a	11/04/98	3312	1970	Ch6E3	1.595 ± 0.003	1.76	8.3 ± 0.4	P0	-0.3 ± 0.3	1.02	-0.32	0.00
30402-01-10-00b	11/04/98	6303	1956	Ch6E3	1.721 ± 0.003	3.86	8.6 ± 0.3	P3	-0.2 ± 0.2	2.25	-0.27	-0.03
30402-01-11-00a	20/04/98	3311	2777	Ch6E3	5.378 ± 0.013	1.92	4.2 ± 0.2	P5	16.0 ± 2.0	0.77	0.97	0.93
30402-01-11-00b	20/04/98	2271	2952	Ch6E3	5.815 ± 0.017	1.75	4.2 ± 0.2	P4	22.5 ± 2.7	2.23	0.89	0.77
30703-01-16-00	28/04/98	5038	1816	Ch6E3	1.382 ± 0.003	2.76	7.1 ± 0.3	P0	-0.0 ± 0.2	0.36	-0.01	-0.11
30703-01-17-00	06/05/98	4584	1739	Ch6E3	0.925 ± 0.002	1.00	8.2 ± 0.5	P0	-0.1 ± 0.1	0.26	-0.58	0.27
30703-01-22-00	27/06/98	3375	1539	Ch6E3	2.256 ± 0.005	1.79	7.5 ± 0.3	P0	-1.1 ± 0.4	0.68	-0.76	0.54
30703-01-25-00a	23/07/98	2626	1718	Ch6E3	3.172 ± 0.007	1.08	7.1 ± 0.4	P4	1.5 ± 0.6	0.76	0.73	0.48
30703-01-25-00b	23/07/98	2322	2146	Ch6E3	3.804 ± 0.009	1.36	5.7 ± 0.3	P5	6.2 ± 0.9	1.15	0.92	0.83
30703-01-33-00	15/09/98	4917	1400	Ch6E3	3.293 ± 0.007	1.07	4.2 ± 0.2	P4	4.3 ± 0.7	4.21	0.76	0.54
30703-01-41-00	26/12/98	4707	1233	Ch6E3	2.158 ± 0.004	1.59	8.7 ± 0.4	P5	0.5 ± 0.3	0.23	0.79	0.58
40403-01-08-00	02/06/99	9884	1584	Ch6E4	2.469 ± 0.003	3.28	7.7 ± 0.2	P1	-1.4 ± 0.2	0.92	-0.92	0.84
40403-01-09-00	08/07/99	13355	1343	Ch6E4	2.041 ± 0.003	2.95	6.6 ± 0.2	P0	-0.3 ± 0.2	0.97	-0.57	0.25
40403-01-11-00	28/02/00	13355	2426	Ch6E4	4.336 ± 0.011	2.88	6.3 ± 0.3	P5	8.0 ± 1.5	0.87	0.83	0.65
40703-01-01-00	01/01/99	9731	1281	Ch6E4	2.265 ± 0.003	1.84	7.0 ± 0.2	P5	0.6 ± 0.2	0.24	0.86	0.71
40703-01-02-00	08/01/99	9005	1861	Ch6E4	3.562 ± 0.005	2.07	4.7 ± 0.1	P4	5.7 ± 0.5	3.19	0.91	0.80
40703-01-05-00	12/02/99	10129	1592	Ch6E4	4.194 ± 0.005	3.17	4.7 ± 0.1	P5	6.9 ± 0.7	1.72	0.94	0.87
40703-01-09-00	28/03/99	4702	1418	Ch6E4	2.782 ± 0.005	1.18	6.5 ± 0.2	P0	0.5 ± 0.4	0.46	0.51	0.17
40703-01-38-02	15/11/99	2501	5138	Ch6E4	7.940 ± 0.034	1.45	5.2 ± 0.5	P5	38.6 ± 4.6	2.18	0.80	0.60
50125-01-01-03	13/07/00	2735	1747	Ch3E5	3.019 ± 0.006	1.98	8.3 ± 0.4	P0	0.7 ± 0.4	1.06	0.44	0.11
50125-01-03-00a	15/07/00	4348	2077	Ch3E5	3.547 ± 0.007	1.77	5.9 ± 0.2	P0	1.3 ± 0.6	1.50	0.47	0.14
50125-01-03-00b	15/07/00	10652	1818	Ch3E5	3.182 ± 0.004	5.37	6.5 ± 0.2	P3	0.4 ± 0.3	2.82	0.22	-0.06
50703-01-01-00	08/03/00	4755	1314	Ch6E4	2.345 ± 0.007	1.34	4.8 ± 0.2	P0	-0.1 ± 0.6	0.99	0.09	-0.10
50703-01-49-00	27/02/01	5467	1434	Ch6E5	2.610 ± 0.004	2.77	8.1 ± 0.3	P0	-0.4 ± 0.3	0.53	-0.47	0.13
50703-01-55-01	17/04/01	6896	1583	Ch6E5	2.840 ± 0.004	2.51	8.4 ± 0.3	P0	-0.6 ± 0.3	0.77	-0.70	0.43
50703-01-67-00	22/07/01	1806	1243	Ch6E5	2.182 ± 0.005	1.57	10.0 ± 0.7	P0	-0.2 ± 0.4	0.17	-0.37	0.04
60100-01-01-00	05/08/01	3280	1249	Ch6E5	2.226 ± 0.004	1.50	12.2 ± 0.6	P1	-0.9 ± 0.3	0.70	-0.83	0.65
60100-01-02-000a	06/08/01	2748	1487	Ch6E5	2.714 ± 0.005	1.29	8.3 ± 0.4	P1	-1.8 ± 0.4	0.47	-0.91	0.82
60100-01-02-000b	06/08/01	2496	1654	Ch6E5	3.021 ± 0.006	1.09	7.2 ± 0.4	P0	-1.4 ± 0.6	0.87	-0.68	0.40
60100-01-02-000c	06/08/01	2648	1762	Ch6E5	3.203 ± 0.007	1.28	6.6 ± 0.3	P0	0.2 ± 0.7	0.49	0.25	-0.04
60100-01-02-000d	06/08/01	2816	1967	Ch6E5	3.515 ± 0.007	1.49	6.7 ± 0.3	P0	1.9 ± 0.7	2.04	0.60	0.28
60100-01-02-000e	06/08/01	2964	2178	Ch6E5	3.839 ± 0.008	2.40	6.4 ± 0.3	P5	4.0 ± 0.9	0.62	0.92	0.84
60405-01-03-00	05/08/01	6560	1474	Ch6E5	2.732 ± 0.004	1.64	8.0 ± 0.3	P1	-0.9 ± 0.3	0.36	-0.88	0.75
60701-01-16-00	28/02/02	3068	1820	Ch6E5	0.377 ± 0.002	0.75	7.2 ± 0.8	P0	-0.0 ± 0.1	0.18	-0.22	-0.06
60701-01-16-01	28/02/02	3109	1809	Ch6E5	0.395 ± 0.002	0.90	7.6 ± 1.2	P0	-0.1 ± 0.1	0.37	-0.52	0.19
60701-01-23-00	22/01/02	3263	1986	Ch6E5	2.082 ± 0.003	3.92	10.3 ± 0.4	P0	-0.5 ± 0.3	1.33	-0.52	0.19
60701-01-28-00	06/03/02	9680	1744	Ch6E5	0.466 ± 0.001	0.99	7.6 ± 0.6	P1	-0.2 ± 0.1	0.76	-0.81	0.63
60701-01-33-00	24/04/02	3247	1426	Ch6E5	1.029 ± 0.002	1.24	10.1 ± 0.8	P0	0.0 ± 0.1	0.60	0.01	-0.11
70702-01-23-00	03/10/02	3231	1931	Ch6E5	3.453 ± 0.005	1.48	9.8 ± 0.4	P1	-2.3 ± 0.5	1.16	-0.80	0.60
70702-01-24-00	09/10/02	3264	1328	Ch6E5	2.581 ± 0.005	2.93	13.2 ± 0.7	P0	-0.3 ± 0.3	0.89	-0.29	-0.02
70703-01-01-08	01/04/02	10704	1902	Ch3E5	2.589 ± 0.004	5.81	7.5 ± 0.2	P0	-0.5 ± 0.3	2.75	-0.53	0.20
70703-01-01-14	29/03/02	8240	1869	Ch6E5	2.639 ± 0.004	5.81	6.2 ± 0.1	P0	-0.4 ± 0.3	2.36	0.24	-0.05
80127-02-03-00	10/04/03	11728	1884	Ch4E5	1.088 ± 0.002	2.84	6.9 ± 0.3	P2	-0.5 ± 0.1	0.86	-0.85	0.69
80701-01-08-00	25/10/06	3216	2375	Ch6E5	4.648 ± 0.012	1.45	6.3 ± 0.3	P5	8.0 ± 1.7	0.43	0.93	0.85
80701-01-26-00	28/11/06	6304	1334	Ch6E5	2.541 ± 0.004	2.72	10.4 ± 0.4	P4	1.2 ± 0.3	1.13	0.71	0.45
80701-01-32-00	04/12/06	1239	1212	Ch6E5	2.104 ± 0.003	1.41	10.3 ± 0.4	P1	-0.6 ± 0.2	0.41	-0.84	0.68
80701-01-51-00	09/12/06	6960	1252	Ch6E5	2.221 ± 0.003	2.14	9.4 ± 0.4	P3	0.3 ± 0.2	1.74	0.16	-0.08
80701-01-55-02	11/01/07	5440	1131	Ch6E5	2.611 ± 0.004	2.16	9.2 ± 0.4	P1	-2.2 ± 0.3	2.28	-0.86	0.71
80701-01-56-00	18/01/07	9600	1073	Ch6E5	2.558 ± 0.001	2.39	16.8 ± 0.6	P0	0.0 ± 0.1	0.52	0.19	-0.07
80701-01-57-00	24/01/07	9584	1100	Ch6E5	2.060 ± 0.003	4.36	13.8 ± 0.5	P5	0.7 ± 0.2	0.31	0.91	0.81

Table 1—Continued

ObsID	Date	GTI[a] (s)	Rate[b]	ChID[c]	QPO			Energy–Frequency				
					Frequency (Hz)	χ^2	Q[d]	P[e]	k^f ($\times 10^{-3}$)	χ^2	R[g]	R2[h]
90105-01-03-01	15/05/04	7152	3023	Ch4E5	4.936 ± 0.009	1.93	5.7 ± 0.2	P0	6.0 ± 1.1	1.74	0.77	0.54
90105-07-01-00	12/04/05	6464	2098	Ch4E5	4.015 ± 0.005	1.46	7.9 ± 0.2	P0	1.5 ± 0.6	1.45	0.41	0.08
90105-07-02-00	13/04/05	6368	2123	Ch4E5	3.895 ± 0.006	2.94	6.8 ± 0.2	P5	3.0 ± 0.6	2.12	0.84	0.66
90701-01-19-00	28/07/04	6416	1200	Ch6E5	2.117 ± 0.002	3.06	13.2 ± 0.5	P1	-0.4 ± 0.1	0.31	-0.90	0.79
91701-01-55-00	02/05/07	9584	1091	Ch6E5	1.986 ± 0.002	2.66	23.7 ± 1.0	P0	-0.4 ± 0.2	0.90	-0.57	0.25
92702-01-09-00	04/05/06	5136	1071	Ch6E5	3.817 ± 0.006	1.17	7.6 ± 0.3	P0	-1.9 ± 0.7	1.03	-0.70	0.43

[a]: Good time interval;

[a]: The unit is cts/s/PCU2;

[c]: ChID is sign which represent the definition of PCA energy bands for light curve extraction listed on Table 2;

[d]: Coherence factor of QPO;

[e]: Pattern of the relation between QPO frequency and photon energy;

[f]: The Least Squares slope;

[g]: Correlation coefficient;

[h]: Adjusted R-square.

Table 2 The Definitions of *RXTE*/PCA Energy Bands for Light Curve Extraction.

ChID[a]	Channel	Energy (keV)	Centroid (keV)	ChID[a]	Channel	Energy (keV)	Centroid (keV)	ChID[a]	Channel	Energy (keV)	Centroid (keV)
Ch1E3	0-13	1.94-5.12	3.53	Ch2E3	0-13	1.94-5.12	3.53	Ch3E3	0-8	1.94-3.35	2.65
	14-18	5.12-6.89	6.01		14-18	5.12-6.89	6.01		9-11	3.35-4.41	3.88
	19-25	6.89-9.39	8.14		19-25	6.89-9.39	8.14		12-13	4.41-5.12	4.77
	26-35	9.39-12.99	11.19		26-35	9.39-12.99	11.19		14-15	5.12-5.82	5.47
	36-41	12.99-15.17	14.08		36-41	12.99-15.17	14.08		16-19	5.82-7.25	6.54
	42-49	15.17-18.09	16.63		42-49	15.17-18.09	16.63		20-23	7.25-8.68	7.97
	50-58	18.09-21.04	19.57						24-29	8.68-10.83	9.76
									30-35	10.83-12.99	11.91
									36-41	12.99-15.17	14.08
									42-47	15.17-17.36	16.27
									48-58	17.36-21.04	19.20
Ch3E5	0-8	2.06-3.68	2.87	Ch4E5	0-8	2.06-3.68	2.87	Ch5E3	0-8	1.94-3.35	2.65
	9-11	3.68-4.90	4.29		9-11	3.68-4.90	4.29		9-11	3.35-4.41	3.88
	12-13	4.90-5.71	5.31		12-13	4.90-5.71	5.31		12-13	4.41-5.12	4.77
	14-15	5.71-6.53	6.12		14-15	5.71-6.53	6.12		14-15	5.12-5.82	5.47
	16-19	6.53-8.17	7.35		16-19	6.53-8.17	7.35		16-19	5.82-7.25	6.54
	20-23	8.17-9.81	8.99		20-23	8.17-9.81	8.99		20-23	7.25-8.68	7.97
	24-29	9.81-12.28	11.05		24-27	9.81-11.45	10.63		24-27	8.68-10.83	9.40
	30-35	12.28-14.76	13.52		28-35	11.45-14.76	13.11		28-35	10.83-12.99	11.55
	36-41	14.76-17.26	16.01		36-39	14.76-16.43	15.60		36-41	12.99-15.17	14.08
	42-47	17.26-19.78	18.52		40-45	16.43-18.94	17.69		42-47	15.17-17.36	16.27
	48-58	19.78-24.00	21.89		46-57	18.94-24.00	21.47		48-58	17.36-21.04	19.20
Ch6E3	0-8	1.94-3.35	2.65	Ch6E4	0-8	2.13-3.79	2.96	Ch6E5	0-8	2.06-3.68	2.87
	9-11	3.35-4.41	3.88		9-11	3.79-5.04	4.42		9-11	3.68-4.90	4.29
	12-13	4.41-5.12	4.77		12-13	5.04-5.88	5.46		12-13	4.90-5.71	5.31
	14-15	5.12-5.82	5.47		14-15	5.88-6.72	6.30		14-15	5.71-6.53	6.12
	16-19	5.82-7.25	6.54		16-19	6.72-8.40	7.56		16-19	6.53-8.17	7.35
	20-23	7.25-8.68	7.97		20-23	8.40-10.09	9.25		20-23	8.17-9.81	8.99
	24-29	8.68-10.83	9.76		24-29	10.09-12.63	11.36		24-29	9.81-12.28	11.05
	30-35	10.83-12.99	11.91		30-35	12.63-15.19	13.91		30-35	12.28-14.76	13.52
	36-39	12.99-14.44	13.72		36-39	15.19-16.90	16.05		36-39	14.76-16.43	15.60
	40-46	14.44-17.00	15.72		40-46	16.90-19.92	18.41		40-46	16.43-19.36	17.90
	47-58	17.00-21.04	19.02		47-58	19.92-24.70	22.31		47-58	19.36-24.00	21.68

[a]: Ch* in ChID represents a definition of PCA energy bands for light curve extraction, and E* in ChID represents the PCA Gain Epoch of the corresponding observations, e.g., Ch3E5 means the third definition in Epoch 5.